Chemical bonding and diffusion of B dopants in C-predoped Si

Sanghun Jwa, Junhyeok Bang, and K. J. Chang

Department of Physics, Korea Advanced Institute of Science and Technology, Daejeon 305-701, Korea
(Received 19 December 2008; revised manuscript received 21 July 2009; published 21 August 2009)

We investigate the atomic structure and electronic properties of various defect configurations which consist of B and C atoms in Si predoped with C impurities through first-principles density-functional calculations. In the absence of Si self-interstitials (I's), substitutional B and C atoms interact repulsively with each other, implying that B-C pairs at neighboring substitutional sites do not behave as a trap for B dopants. For I-B-C complexes, which can be formed in the presence of self-interstitials, we find that a C-B split interstitial, where the B and C atoms share a single lattice site along the [001] axis, is the most stable configuration. For several diffusion pathways, along which the B dopant diffuses from the C-B split-interstitial configuration with the [001] orientation to nearby tetrahedral and hexagonal sites, we find very high migration energies of about 3 eV. Thus, the diffusing B atom can be easily trapped in the neighborhood of C, resulting in the reduction in the B diffusivity. The range of the C trap potential is estimated to be about 7 Å. We also examine the diffusion of C from the stable C-B split interstitial, leaving the B dopant at a substitutional site, and find the migration energy to be much reduced to 2.16 eV. This result indicates that, as the C atom is dissociated, it acts as a trap for self-interstitials, leading to the reduction in self-interstitials which are available for B diffusion. In this case, the suppression of the B diffusivity is still expected, without degrading the electrical activity of the B dopants.

PACS number(s): 61.72.uf, 66.30.J−, 71.55.−i, 85.40.Ry

I. INTRODUCTION

The size of metal-oxide-semiconductor devices has been scaled down exponentially following Moore's Law, reaching the spatial scale of sub 0.1 μm.[1] The development of Si-based integrated circuit technology keeps demanding the reduction in device size and the improvement of efficiency. One of the challenging issues in Si device technology is the formation of ultrashallow *pn* junctions. To this end, thermal annealing and dopant diffusion have attracted much attention. In case of B, which is widely used as a *p*-type dopant, B diffusivity is known to be enhanced under nonequilibrium conditions after ion implantation and subsequent thermal annealing.[2–4] This phenomenon is called boron transient-enhanced diffusion (TED) and believed to be caused by the supersaturation of Si self-interstitials (I's).[5,6] In this case, Si self-interstitials play a crucial role in the B diffusion which can be proceeded via either the kick-out mechanism or the interstitialcy mechanism. In the kick-out mechanism, a substitutional B is kicked out by a self-interstitial and then migrates as an interstitial until it is kicked in other substitutional Si.[7–9] On the other hand, several theoretical calculations have suggested that the interstitialcy mechanism is energetically more tenable, in which a substitutional B diffuses with keeping the formation of a pair with the self-interstitial.[10–12]

During the TED of dopants, lateral broadening of source-drain junctions occurs, which in turn causes the degradation of device performance. Thus, it is important to control and reduce the dopant diffusion in Si-based technology. Experimentally, several approaches have been proposed to reduce B diffusivity in which other species are incorporated into the Si lattice along with B dopants. In Si predoped with donor dopants, the reduction in B diffusivity was attributed to the formation of donor-acceptor pairs which act as a trap for B.[13–16] For P dopants, the migration energy for B diffusion was shown to increase by about 0.2 eV in the presence of P.[17] The retardation of B diffusion was also observed in SiGe

alloys.[18–21] Although the strain effect was considered to be the origin of the retarded B diffusion, experimental and theoretical results on the strain effect on B diffusion are quite controversial.[20–22] In other first-principles calculations, the retarded B diffusion by the presence of Ge was attributed to two major effects, the decrease in self-interstitials available for B diffusion and the increase in the B migration energy.[23,24] It was reported that the TED of B can be suppressed by incorporation of substitutional C atoms.[25,26] Theoretically, it is agreed that substitutional C acts as a trap for self-interstitials, which are available for the B TED, resulting in the undersaturation of self-interstitials.[27–29] It was further suggested that the formation of C-B split-interstitial configurations is additionally responsible for the suppression of B diffusivity.[28] In amorphous Si, although the reduction in B diffusivity by C codoping was not found, a concomitant reduction in B clustering was observed, suggesting that C acts as a trap for B dopants.[30] First-principles calculations showed that the migration energy for B diffusion is enhanced by about 0.38 eV in the presence of C.[31] However, in this study, only the diffusion pathway of B along hexagonal and tetrahedral sites was considered in the neighborhood of substitutional C and the effect of self-interstitial was not taken into account. Moreover, the chemical-bonding effect of C on B diffusion and the actual diffusion pathway of B in the presence of self-interstitial have not been studied yet.

In this work, we study the atomic structure and energetics of various defect configurations consisting of C, B, and Si self-interstitial in Si through first-principles pseudopotential calculations. We examine the diffusion pathways of B and C from the stable defect configuration and the chemical-bonding effect of C on B diffusion under two different conditions where self-interstitials are absent and abundant. Based on the results for the formation and migration energies, we discuss the role of C on the suppression of B diffusivity in C-predoped Si.

II. CALCULATION METHOD

The total energies and wave functions are calculated using the pseudopotential method within the density-functional theory,[32] as implemented in the VASP code.[33] We employ the generalized gradient approximation (GGA) (Ref. [34]) for the exchange-correlation potential and ultrasoft pseudopotentials[35] for the ionic potentials. We use a plane-wave basis to expand the wave functions, with a cutoff energy of 287 eV, which ensures the accuracy of total energies to within a few tens of meV. We choose a cubic supercell containing 64 host atoms to study the atomic and electronic properties of C- and B-related defects and the diffusion of the dopant atom. We test a larger supercell containing 216 host atoms and find that the formation and migration energies are accurate to within 0.1 eV. To calculate the potential range of the C atom over which the B diffusion is affected, we use a 128-atom supercell which is made by choosing two 64-atom supercells along one cubic axis. Thus, interactions between the B and C atoms in neighboring supercells are prohibited. The lattice constant of 5.457 Å, which is calculated by the GGA, is used for supercell calculations. The Brillouin-zone integration of the charge densities is performed using a set of uniform **k** points generated by the $3 \times 3 \times 3$ and $1 \times 3 \times 3$ Monkhorst-Pack meshes[36] for supercells with 64 and 128 host atoms, respectively. The ionic positions are fully relaxed using the conjugate gradient method until residual forces are less than 0.01 eV/Å. For charged defects, we use a jellium background that neutralizes the charged unit cell and thereby prevents the Coulomb interaction from being divergent. Both the nudged elastic band (NEB) and dimer methods[37,38] are used to find the diffusion pathway and migration energy for B diffusion. Although the dimer method is more efficient in finding a saddle point, it often gives other saddle point which does not lie along the pathway because it uses information on two adjacent images. On the other hand, the NEB method gives a more accurate pathway but it is time consuming because more images are needed. In our calculations, we first use the NEB method to extract a diffusion pathway with initial images generated by linear interpolation between initial and final configurations, and then employ the dimer method to find a well-converged transition state.

The formation energy (E_f) of a defect D in neutral charge state is defined as[12,39]

$$E_f(D) = E_{tot}(D) - E_{bulk}(\text{Si}) - \sum_i \mu_i[n_i(D) - n_i^{(0)}], \quad (1)$$

where $E_{tot}(D)$ is the total energy of a supercell containing the defect D whereas $E_{bulk}(\text{Si})$ is the total energy of the perfect supercell without any defects and impurities. Here $n_i(D)$ and μ_i are the number of species i ($i=$Si, C, and B) in the supercell containing the defect D and the corresponding reservoir chemical potential, respectively. On the other hand, $n_i^{(0)}$ denotes the number of species i in the perfect supercell. The chemical potentials, μ_C (μ_B) and μ_{Si}, are calculated from the energy of a substitutional C (B) atom in Si and the total energy per atom of perfect Si, respectively. Then, for a defect complex which consists of the B and C atoms, $E_f(D)$ repre-

sents the energy required to form the defect from isolated substitutional C and B atoms.

III. RESULTS AND DISCUSSION

A. Atomic and electronic structure of B-related defects

We first examine the stability of a B-C complex in the absence of Si self-interstitials. As the C atom is isoelectronic to the Si lattice, it is likely to be positioned at a substitutional site without altering the charge state of B. For a substitutional C (C_s), the Si atoms at the first-neighbor distance undergo large inward relaxations of 0.33 Å toward the C atom due to the smaller atomic radius than that of the Si atom. Similarly, we find inward relaxations of 0.27 Å for the Si atoms surrounding a substitutional B (B_s). When the B and C atoms form a B_s-C_s pair, inward relaxations of the neighboring Si atoms are enhanced, increasing strains around the pair. The energies of the B_s-C_s pair in neutral (1−) charge state with respect to two isolated C and B atoms are calculated to be 0.72 (0.66), 0.19 (0.13), and 0.17 (0.10) eV at the first-, second-, and third-neighbor distances, respectively, indicating that the B and C atoms repel to each other. As the formation of B_s-C_s pairs is energetically unfavorable, the C atoms do not behave as a trap for B dopants.

Under nonequilibrium conditions after ion implantation and rapid thermal annealing, it is known that the diffusivity of B dopants is greatly enhanced with the aid of self-interstitials. It is understood that a substitutional B forms an I-B_s pair with a nearby self-interstitial, which is positioned at a tetrahedral site, and diffuses without pair dissociation, especially in the interstitialcy diffusion.[10–12] If the C atoms are introduced into the Si lattice, a diffusing B dopant can be trapped by forming an I-B-C complex with the C atom. To find the stable I-B-C complex, we consider various configurations (Fig. 1) and compare their formation energies in Table I. In I-B_s-C_s configurations, where the substitutional C and B atoms are positioned at the first-neighbor distance, four tetrahedral sites [labeled 1, 2, 3, and 4 in Fig. 1(a)] are available for the position of the self-interstitial. As the neighboring Si atoms undergo large inward relaxations of about 0.078 Å even in the presence of the self-interstitial, the formation energies are relatively high, being 3.60, 3.34, 3.60, and 3.75 eV at sites 1, 2, 3, and 4, respectively. During the interstitialcy diffusion, it is likely for the B dopant to diffuse from its substitutional site to a nearby interstitial site [labeled 1, 2, and 3 in Fig. 1(b)], resulting in a B_i-C_s configuration, in which the self-interstitial substitutes for the substitutional B. As the relaxations of the neighboring Si atoms are reduced to 0.067 Å, the formation energies of the B_i-C_s configurations are lowered to 3.02, 2.61, and 2.88 eV, respectively, for the tetrahedral and hexagonal B atoms, which are positioned at sites labeled 1, 2, and 3 in Fig. 1(b). For B in SiC, previous calculations showed that a hexagonal position is the most stable configuration for B,[40,41] while the formation energy of the hexagonal B is very high in C-predoped Si.

We examine split-interstitial configurations in which either the B or C atom forms a dumbbell-like structure sharing a single lattice site with the host Si atom. Figures 1(c) and 1(d) show the atomic structures of C_s-$(B\text{-}I)_{split}^{[110]}$ and
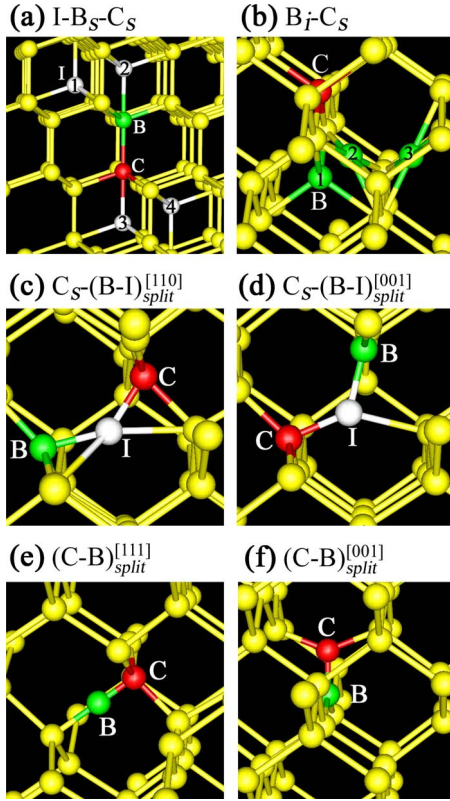
(a) I-B$_S$-C$_S$

(b) B$_i$-C$_S$

(c) C$_S$-(B-I)$^{[110]}_{split}$

(d) C$_S$-(B-I)$^{[001]}_{split}$

(e) (C-B)$^{[111]}_{split}$

(f) (C-B)$^{[001]}_{split}$

FIG. 1. (Color online) The atomic structures of the (a) I-B$_s$-C$_s$, (b) B$_i$-C$_s$, (c) C$_s$-(B-I)$^{[110]}_{split}$, (d) C$_s$-(B-I)$^{[001]}_{split}$, (e) (C-B)$^{[111]}_{split}$, and (f) (C-B)$^{[001]}_{split}$ configurations. Numbers in (a) and (b) denote possible positions of I and B$_i$, respectively. The Si, C, and B atoms are represented by yellow (unlabeled white balls in print), red, and green balls, respectively.

C$_s$-(B-I)$^{[001]}_{split}$, in which the B and self-interstitial atoms sharing a lattice site are directed along the [110] and [001] axes, respectively, and the C atom is positioned at a nearby substitutional site. Although these configurations induce large relaxations of about 0.075 Å for the neighboring Si atoms, their formation energies of 1.46 and 1.87 eV are found to be much lower than those for I-B$_s$-C$_s$ and B$_i$-C$_s$. For other configurations, in which the C and self-interstitial atoms share a single lattice site, with the B atom positioned at a nearby substitutional site, we find similar formation energies of 1.06 and 1.51 eV for the [001] and [110] orientations, respectively (Table I).

When the C and B atoms form split-interstitial configurations, the formation energies are significantly reduced due to small relaxations of about 0.056 Å induced for the neighboring Si atoms. Among the split-interstitial configurations considered here, the lowest-energy state is found to be the (C-B)$^{[001]}_{split}$ configuration with the formation energy of 0.29 eV, in good agreement with previous calculations.[28] In this configuration, the C and B atoms in the sp^2-type bonding state are directed along the [001] axis [Fig. 1(f)]. For the (C-B)$^{[111]}_{split}$ configuration, the formation energy is calculated to be 0.83 eV when the B atom is positioned at a bond-centered site along the [111] axis [Fig. 1(e)], while it increases to 1.11 eV for the case of the C atom at a bond-centered site. On the other hand, the split-interstitial configuration with the [110] orientation is found to be unstable. We test the accuracy of our calculations by using a lager supercell containing 216 host atoms, and find that the formation energy of (C-B)$^{[001]}_{split}$ increases only by 0.07 eV, whereas those for the (C-B)$^{[111]}_{split}$ configurations increase by 0.08–0.09 eV. Thus, the energy differences between different configurations are accurate to within 0.1 eV.

In the diffusion process of an I-B$_s$ pair via the interstitialcy mechanism, the B dopant can be trapped by a substitutional C via the formation of (C-B)$^{[001]}_{split}$ which is energetically the most stable configuration. Before (C-B)$^{[001]}_{split}$ is formed, one may expect that either I-B$_s$-C$_s$, B$_i$-C$_s$, or C$_s$-(B-I)$_{split}$ can be an intermediate configuration. However, C$_s$-(B-I)$_{split}$ is more likely to be formed than I-B$_s$-C$_s$ and B$_i$-C$_s$ because it has the lower formation energies (Table I). It is noted that C$_s$-(B-I)$_{split}$ can be transformed into (C-B)$^{[001]}_{split}$ by rotating either the I-B or I-C bond [Figs. 1(c) and 1(d)]. We find the reaction, C$_s$+(I-B$_s$)→(C-B)$^{[001]}_{split}$, to be exothermic with the energy lowered by 2.32 eV. In the absence of the B dopant, a self-interstitial is also trapped by the C atom, following the reaction, C$_s$+I→(C-I)$^{[001]}_{split}$. In this case, the exothermic energy is found to be 1.80 eV, in good agreement with previous calculations.[28] When (C-I)$^{[001]}_{split}$ diffuses and forms the (C-B)$^{[001]}_{split}$ configuration with a substitutional B, the energy decreases by 1.69 eV. Thus, our calculations indicate that incorporated C atoms trap not only self-interstitials but also the B dopants which diffuse in the form of I-B$_s$ pairs.

The atomic structure of (C-B)$^{[001]}_{split}$ is very similar to that of the (C-I)$^{[001]}_{split}$ defect, which was shown to be the most stable form of an interstitial C sharing a single lattice site with the host atom in the absence of B.[42] The defect-related energy

TABLE I. Comparison of the formation energies (in units of eV) of various defect configurations which consist of the self-interstitial (I), C, and B atoms. Numbers in the I-B$_s$-C$_s$ and B$_i$-C$_s$ configurations denote the positions of I and B$_i$ in Figs. 1(a) and 1(b), respectively, and three orientations along the [001], [110], and [111] directions are considered for split-interstitial configurations.

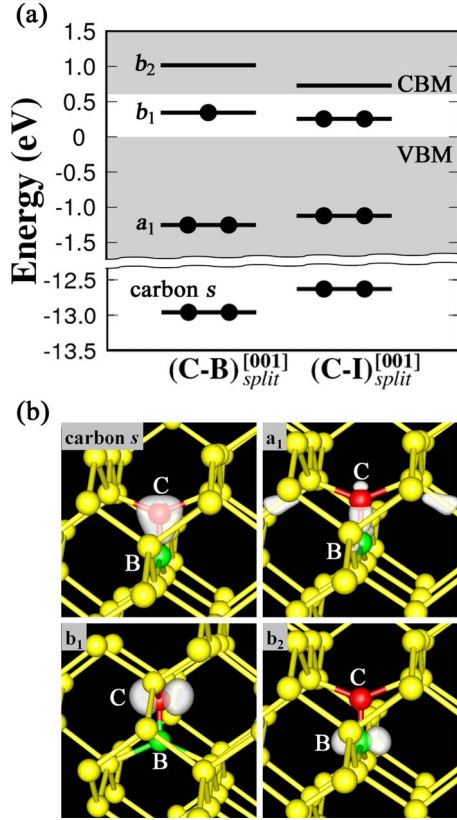| Configuration	1	2	3	4	[001]	[110]	[111]
I-B$_s$-C$_s$	3.60	3.34	3.60	3.75			
B$_i$-C$_s$	3.02	2.61	2.88				
C$_s$-(B-I)$_{split}$					1.87	1.46	
B$_s$-(C-I)$_{split}$					1.06	1.51	
(C-B)$_{split}$					0.29		0.83

FIG. 2. (Color online) (a) Four defect levels of $(C\text{-}B)_{split}^{[001]}$ are compared with those for $(C\text{-}I)_{split}^{[001]}$ in pure Si. (b) The isosurfaces of electronic charge densities are plotted for the C s-derived level and the a_1, b_1, and b_2 defect levels of $(C\text{-}B)_{split}^{[001]}$.
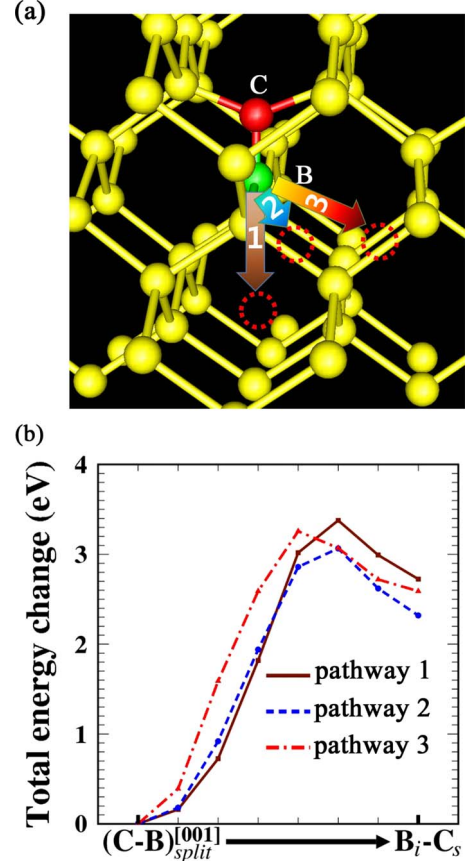

FIG. 3. (Color online) (a) Three possible diffusion pathways for the B dopant from $(C\text{-}B)_{split}^{[001]}$ are labeled 1, 2, and 3, which correspond to the final configurations in which the B atom is positioned at the first-nearest tetrahedral, first- and second-nearest hexagonal sites, respectively. (b) The variations in the energies are plotted for B diffusion along the three diffusion pathways.

levels of $(C\text{-}B)_{split}^{[001]}$ and $(C\text{-}I)_{split}^{[001]}$ are identified by examining the charge densities of all the energy states. Due to the structural similarity, we find that the defect levels of $(C\text{-}B)_{split}^{[001]}$ are similar to those for $(C\text{-}I)_{split}^{[001]}$, as shown in Fig. 2(a). The defect levels with b_1 and b_2 symmetries correspond to non-bonding p orbitals on the C and B atoms, respectively [Fig. 2(b)]. The highest-occupied b_1 level is located in the band gap while the unoccupied b_2 level lies in the conduction band. The b_1 and b_2 levels of $(C\text{-}B)_{split}^{[001]}$ are higher by 0.08 and 0.29 eV, respectively, as compared to the $(C\text{-}I)_{split}^{[001]}$ configuration. The doubly occupied a_1 level is positioned at about -1.2 eV below the valence-band maximum, and the energy level derived from the C s orbital is much lower, lying around -13.0 eV. The charge densities of the a_1 level are mainly localized in the bonding region between the C and B atoms while they are distributed over the Si atoms neighboring the C atom in the $(C\text{-}I)_{split}^{[001]}$ configuration.[42] As the size of the B atom is smaller than that of the Si atom, outward relaxations of the neighboring Si atoms are smaller in the $(C\text{-}B)_{split}^{[001]}$ configuration. Due to the reduced strain, the a_1 and C s-derived levels of $(C\text{-}B)_{split}^{[001]}$ are lower by 0.13 and 0.33 eV, respectively, resulting in the lowest-energy configuration. In addition, the localized defect levels of $(C\text{-}B)_{split}^{[001]}$ cause degradation in B activation, as observed in C-implanted Si.[43]

B. B and C diffusions from the $(C\text{-}B)_{split}^{[001]}$ configuration

To see how strongly the B dopant is trapped by the C atom, we examine various diffusion processes. In Si, previous studies have suggested that the B diffusion is proceeded via the interstitialcy mechanism which is primarily mediated by self-interstitials.[10–12] In SiC, the main diffusion process of B is very different from that found in Si, following a kick-out mechanism, where the B dopant is first kicked out by a nearby self-interstitial and then diffuses as an interstitial.[40,41,44,45] In C-predoped Si, we consider a diffusion process in which a $(C\text{-}B)_{split}^{[001]}$ configuration transforms into an I-B_s-C_s configuration via the kick-out mechanism and then the B atom diffuses with the aid of a self-interstitial, following the interstitialcy mechanism. However, this diffusion process is likely to be suppressed because the formation energies of I-B_s-C_s are very high, as shown in Table I. In other diffusion process [Fig. 3(a)], the B atom initially forms the stable $(C\text{-}B)_{split}^{[001]}$ configuration and then migrates into a nearby interstitial site, maintaining a C-B pair with the C atom which eventually occupies a substitutional site. For three diffusion pathways labeled 1, 2, and 3, the calculated formation energies are compared in Fig. 3(b). The migration energy, which is given by the energy difference between the
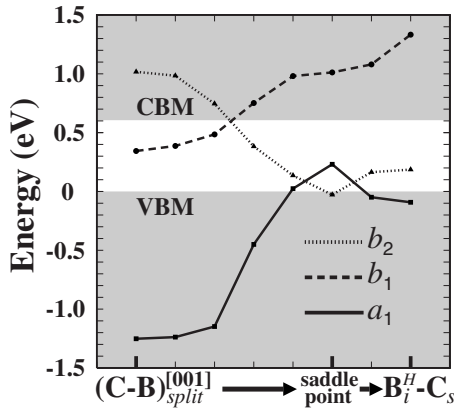
FIG. 4. The variations in the a_1, b_1, and b_2 defect levels are drawn when B diffuses from the $(C\text{-}B)_{split}^{[001]}$ configuration into the interstitial B positioned at the first-nearest hexagonal site along the diffusion pathway 1 in Fig. 3(a).

$(C\text{-}B)_{split}^{[001]}$ and saddle-point configurations, is found to be 3.38 eV for the diffusion pathway 1 into a nearest tetrahedral site. For the pathways 2 and 3, along which the B atom migrates into the first- and second-neighboring hexagonal sites, the migration energies are calculated to be 3.07 and 3.26 eV, respectively. Using the 216-atom supercell, we obtain the migration energy of 3.02 eV for the pathway 2, which ensures the accuracy of calculations to within 0.1 eV.

When the B dopant in the final configuration [Fig. 3(b)] further moves away from the substitutional C, the B diffusion will be proceeded in the form of the I-B_s pair. In this case, as the energy of isolated C_s and I-B_s is higher by 2.32 eV than that of $(C\text{-}B)_{split}^{[001]}$, this energy difference can be considered as the lower bound for the migration energy. Thus, for the B diffusion from the $(C\text{-}B)_{split}^{[001]}$ configuration, the overall migration energy is considerably higher than the value of about 0.4 eV for B diffusion in pure Si.[10–12] Even in the presence of P or Ge impurities, which result in the reduction in B diffusivity in P-predoped Si and SiGe alloys, the migration energies were shown to increase only by about 0.2 eV.[17,23] Due to the high migration energy for B diffusion, the C atom behaves as a trap for the B dopant, indicating that the $(C\text{-}B)_{split}^{[001]}$ configuration plays a role in the suppression of B diffusivity.

The effect of the C atom on the migration energy is examined by analyzing the defect levels during the B diffusion process. The variations in the a_1, b_1, and b_2 levels are drawn along the diffusion pathway 1 in Fig. 4. As the B atom diffuses from the $(C\text{-}B)_{split}^{[001]}$ configuration, the singly occupied b_1 level moves to higher energies above the conduction-band minimum. The unoccupied b_2 level gradually decreases to the top of the valence band and eventually lies in the band gap. Thus, the occupied defect level changes from b_1 to b_2 before the B dopant reaches the saddle point. In the meantime, as the C-B bond is weakened, the a_1 level rapidly increases, with a highest value in the band gap at the saddle point. The variation in the formation energy in Fig. 3(b) is very similar to that of the a_1 level. As the population of the a_1 level is twice that of the b_1 or b_2 level, the variation in the a_1 level, which corresponds to the bonding between the C
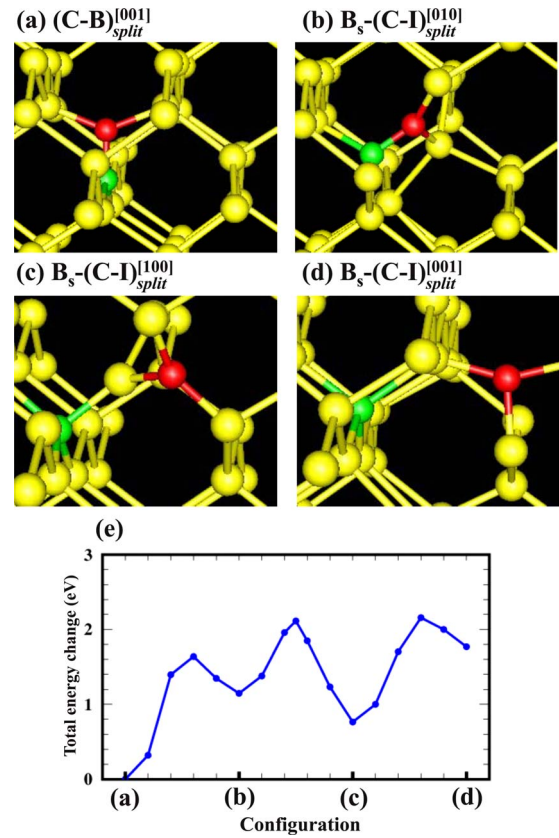

FIG. 5. (Color online) The C atom, which initially forms the (a) $(C\text{-}B)_{split}^{[001]}$ configuration, diffuses into the (d) $B_s\text{-}(C\text{-}I)_{split}^{[001]}$ configuration via the intermediate configurations of (b) $B_s\text{-}(C\text{-}I)_{split}^{[010]}$ and (c) $B_s\text{-}(C\text{-}I)_{split}^{[100]}$. (e) The variation in the energy is plotted along the diffusion pathway of the C atom.

and B atoms, plays an important role in determining the migration barrier on the diffusion pathway.

Finally we consider a diffusion process, in which the C atom diffuses from the stable $(C\text{-}B)_{split}^{[001]}$ configuration to a neighboring site, while the B dopant keeps a substitutional configuration. For the $(C\text{-}I)_{split}^{[001]}$ configuration, previous calculations showed that the C atom easily diffuses to a nearby substitutional site with the energy barrier of about 0.51 eV, changing its orientation from [001] to [010] or [100].[46] In the case of $(C\text{-}B)_{split}^{[001]}$, the diffusion pathway of C is strongly affected by the presence of the B dopant. When the C atom first diffuses to one of the neighboring Si atoms, the final state is a $(C\text{-}I)_{split}$ configuration with the [010] orientation [Fig. 5(b)], and the reaction barrier is calculated to be about 1.64 eV [Fig. 5(e)]. If $(C\text{-}I)_{split}^{[010]}$ further diffuses along the [110] pathway, it changes the orientation from [010] to [100] at the same lattice site [Fig. 5(c)] and then turns into a $(C\text{-}I)_{split}$ configuration with the [001] orientation at a nearby site [Fig. 5(d)]. In these reorientation and diffusion processes, the reaction barriers are found to be 0.97 and 1.39 eV, respectively. The overall reaction barrier for the C diffusion is 2.16 eV, which is lower by about 0.90 eV than that for the B diffusion, indicating that the C atom is more likely to be dissociated from the $(C\text{-}B)_{split}^{[001]}$ configuration than the B dopant does. The dissociation process of C does not degrade the
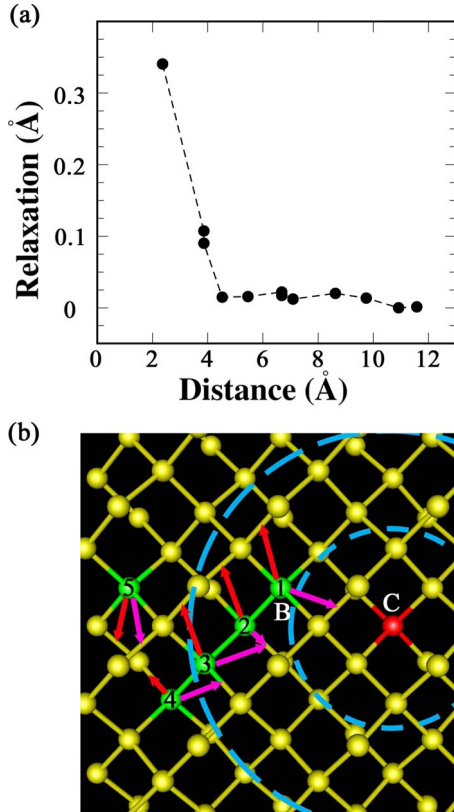
FIG. 6. (Color online) (a) Inward relaxations of the Si atoms around a substitutional C are drawn as a function of the distance between the C and Si atoms. (b) Numbers denote five different positions of the B dopant, which initially forms an I-B_s pair with the self-interstitial, in the vicinity of the substitutional C. Arrows in different colors denote inward and outward directions of the B diffusion relative to the C atom. Small and large dashed circles represent distances of 4 and 7 Å, respectively, from the C atom.

electrical activity of the B dopant because the B atom remains at a substitutional site while $(C-B)_{split}^{[001]}$ is electrically inactive. In addition, as the self-interstitial is trapped by the dissociated C atom, the presence of C eventually leads to the reduction in self-interstitials, which are available for the B diffusion. Thus, even if the C atom is dissociated from the $(C-B)_{split}^{[001]}$ configuration, the B diffusivity is still expected to be suppressed, as previously suggested.[27–29]

C. Effective range of the C atom on B diffusion

Due to the small atomic radius, the C atom induces large inward relaxations for the neighboring Si atoms, as discussed earlier. The inward relaxations of the Si atoms surrounding a single substitutional C are plotted as a function of the distance between the C and Si atoms in Fig. 6(a). The Si atoms within the distance of about 4 Å undergo large relaxations while the Si displacements are less than 0.025 Å for distances above 4 Å. Thus, the distortion range of the Si lattice by a substitutional C is roughly estimated to be about 4 Å. To see whether the C atom indeed acts as a trap for the diffusing B atom, we examine the range of the C trap potential. We assume that the B dopant, which is positioned at a

TABLE II. Comparison of the energies of two final configurations, in which the B atom is located at different hexagonal sites after diffusing from the I-B_s pair, for various initial positions of the substitutional B in Fig. 6(b). Here $d_{initial}$ and d_{final} denote the distances between the B and C atoms before and after the B diffusion, respectively, and ΔE represents the increase in the energy in the final configuration of the B dopant with respect to the initial configuration.

Initial B position	$d_{initial}$ (Å)	d_{final} (Å)	ΔE (eV)
1	4.48	2.80	0.18
		6.59	0.37
2	5.41	5.21	0.41
		6.50	0.46
3	7.02	5.21	0.40
		7.85	0.44
4	8.57	6.50	0.43
		9.32	0.45
5	9.77	8.93	0.45
		10.50	0.46

substitutional site far from the substitutional C, initially forms an I-B_s pair with the self-interstitial at a nearby tetrahedral site. The B atom of the I-B_s pair can diffuse either toward or away from the C atom with the help of the self-interstitial via the kick-out or interstitialcy mechanism. For each B substitutional [labeled 1–5 in Fig. 6(b)], we compare the formation energies of two final configurations (Table II), in which the B atom is positioned at a hexagonal site after traveling an average distance of about 2.25 Å along the toward or outward diffusion pathway. Although we did not calculate the migration barriers for all the diffusion pathways, we are able to find a tendency that the B atom is likely to diffuse toward the C atom for distances smaller than 7 Å between the B and C atoms. However, for distances larger than 7 Å, we find very small energy differences less than 0.02 eV between the two final configurations, indicating that there is no preferential direction for the B diffusion. Thus, the C trap potential is effective to the B dopant within the distance of about 7 Å.

IV. CONCLUSIONS

In conclusion, we have investigated the effect of the C atom on the chemical bonding and diffusion of the B dopant in Si through the first-principles pseudopotential calculations. The C atoms incorporated into the Si lattice interact repulsively with the B dopants in the absence of Si self-interstitials. Among various defect configurations which consist of the self-interstitial, B and C atoms, the $(C-B)_{split}^{[001]}$ configuration, where the B and C atoms form a dumbbell-like structure at a single lattice site, is found to be energetically most stable, in good agreement with previous calculations.[28] For several diffusion pathways of the B dopant from the $(C-B)_{split}^{[001]}$ configuration, we find that the presence of C in-

creases significantly the migration energy to about 3 eV, compared with the value of about 0.4 eV for B diffusion in pure Si and even the migration barriers of about 0.6–0.8 eV in P- and Ge-predoped Si. Thus, the C atom can act as a trap for the B dopants, which diffuse with the aid of self-interstitials, via the formation of the $(C\text{-}B)^{[001]}_{split}$ configuration. When the C atom is dissociated from the $(C\text{-}B)^{[001]}_{split}$ configuration, the migration energy is reduced to 2.16 eV, indicating that the C atom is more easily dissociated. In this case, the self-interstitial, which initially forms a complex with the B

dopant, is eventually trapped by the dissociated C atom. Our calculations indicate that, in C-predoped Si, the suppression of the B diffusivity is due to the formation of the $(C\text{-}B)^{[001]}_{split}$ configuration and the reduction in self-interstitials available for the B diffusion.

[1] The International Technology Roadmap for Semiconductors, Emerging Research Devices, 2004 (http://public.itrs.net).

[2] A. E. Michel, W. Rausch, P. A. Ronsheim, and R. H. Kastl, Appl. Phys. Lett. **50**, 416 (1987).

[3] M. Servidori, Z. Sourek, and S. Solmi, J. Appl. Phys. **62**, 1723 (1987).

[4] P. Pichler and D. Stiebel, Nucl. Instrum. Methods Phys. Res. B **186**, 256 (2002).

[5] D. J. Eaglesham, P. A. Stolk, H.-J. Gossmann, and J. M. Poate, Appl. Phys. Lett. **65**, 2305 (1994).

[6] *Defects and Diffusion in Silicon Processing*, edited by S. Coffa, T. Diaz de la Rubia, P. A. Stolk, and C. S. Rafferty, MRS Symposia Proceedings No. 469 (Materials Research Society, Warrendale, 1997).

[7] R. Car, P. J. Kelly, A. Oshiyama, and S. T. Pantelides, Phys. Rev. Lett. **54**, 360 (1985).

[8] C. S. Nichols, C. G. Van de Walle, and S. T. Pantelides, Phys. Rev. Lett. **62**, 1049 (1989).

[9] J. Zhu, T. Diaz de la Rubia, L. H. Yang, C. Mailhiot, and G. H. Gilmer, Phys. Rev. B **54**, 4741 (1996).

[10] W. Windl, M. M. Bunea, R. Stumpf, S. T. Dunham, and M. P. Masquelier, Phys. Rev. Lett. **83**, 4345 (1999).

[11] B. Sadigh, T. J. Lenosky, S. K. Theiss, M.-J. Caturla, T. Diaz de la Rubia, and M. A. Foad, Phys. Rev. Lett. **83**, 4341 (1999).

[12] J.-W. Jeong and A. Oshiyama, Phys. Rev. B **64**, 235204 (2001).

[13] S. Solmi and S. Valmorri, J. Appl. Phys. **77**, 2400 (1995).

[14] E. G. Tishkovskii, V. I. Obodnikov, A. A. Taskin, K. V. Feklistov, and V. G. Seryapin, Semiconductors **34**, 629 (2000).

[15] S. Solmi and M. Bersani, J. Appl. Phys. **87**, 3696 (2000).

[16] B. Margesin, R. Canteri, S. Solmi, A. Armigliato, and F. Baruffaldi, J. Mater. Res. **6**, 2353 (1991).

[17] C.-Y. Moon, Y.-S. Kim, and K. J. Chang, Phys. Rev. B **69**, 085208 (2004).

[18] P. Kuo, J. L. Hoyt, J. F. Gibbons, J. E. Turner, R. D. Jacowitz, and T. I. Kamins, Appl. Phys. Lett. **62**, 612 (1993).

[19] N. E. B. Cowern, P. C. Zalm, P. van der Sluis, D. J. Gravesteijn, and W. B. de Boer, Phys. Rev. Lett. **72**, 2585 (1994).

[20] P. Kuo, J. L. Hoyt, J. F. Gibbons, J. E. Turner, and D. Lefforge, Appl. Phys. Lett. **66**, 580 (1995).

[21] N. R. Zangenberg, J. Fage-Pedersen, J. L. Hansen, and A. N. Larsen, J. Appl. Phys. **94**, 3883 (2003).

[22] L. Lin, T. Kirichenko, B. R. Sahu, G. S. Hwang, and S. K. Banerjee, Phys. Rev. B **72**, 205206 (2005).

[23] J. Bang, J. Kang, W.-J. Lee, K. J. Chang, and H. Kim, Phys. Rev. B **76**, 064118 (2007).

[24] L. Wang, P. Clancy, and C. S. Murthy, Phys. Rev. B **70**, 165206 (2004).

[25] P. A. Stolk, D. J. Eaglesham, H.-J. Gossmann, and J. M. Poate, Appl. Phys. Lett. **66**, 1370 (1995).

[26] H. Rücker, B. Heinemann, W. Röpke, R. Kurps, D. Krüger, G. Lippert, and H. J. Osten, Appl. Phys. Lett. **73**, 1682 (1998).

[27] R. Scholz, U. Gösele, J.-Y. Huh, and T. Y. Tan, Appl. Phys. Lett. **72**, 200 (1998).

[28] C.-L. Liu, W. Windl, L. Borucki, S. Lu, and X.-Y. Liu, Appl. Phys. Lett. **80**, 52 (2002).

[29] A. Mattoni, F. Bernardini, and L. Colombo, Phys. Rev. B **66**, 195214 (2002).

[30] L. A. Edelman, S. Jin, K. S. Jones, R. G. Elliman, and L. M. Rubin, Appl. Phys. Lett. **93**, 072107 (2008).

[31] H. Li, P. Kohli, S. Ganguly, T. A. Kirichenko, and P. Zeitzoff, Appl. Phys. Lett. **77**, 2683 (2000).

[32] P. Hohenberg and W. Kohn, Phys. Rev. **136**, B864 (1964); W. Kohn and L. J. Sham, *ibid.* **140**, A1133 (1965).

[33] G. Kresse and J. Hafner, Phys. Rev. B **47**, 558 (1993); G. Kresse and J. Furthmüller, *ibid.* **54**, 11169 (1996).

[34] J. P. Perdew, K. Burke, and M. Ernzerhof, Phys. Rev. Lett. **77**, 3865 (1996).

[35] D. Vanderbilt, Phys. Rev. B **41**, 7892 (1990).

[36] H. J. Monkhorst and J. D. Pack, Phys. Rev. B **13**, 5188 (1976).

[37] H. Jonsson, G. Mills, and K. W. Jacobsen, in *Classical and Quantum Dynamics in Condensed Phase Simulations*, edited by B. J. Berne, G. Ciccotti, and D. F. Coker (World Scientific, Singapore, 1998), p. 385.

[38] B. W. H. van Beest, G. J. Kramer, and R. A. van Santen, Phys. Rev. Lett. **64**, 1955 (1990).

[39] M. Hakala, M. J. Puska, and R. M. Nieminen, Phys. Rev. B **61**, 8155 (2000).

[40] R. Rurali, P. Godignon, J. Rebollo, P. Ordejón, and E. Hernández, Appl. Phys. Lett. **81**, 2989 (2002).

[41] R. Rurali, E. Hernández, P. Godignon, J. Rebollo, and P. Ordejón, Phys. Rev. B **69**, 125203 (2004).

[42] P. Leary, R. Jones, S. Öberg, and V. J. B. Torres, Phys. Rev. B **55**, 2188 (1997).

[43] I. Ban, M. C. Öztürk, K. Christensen, and D. M. Maher, Appl. Phys. Lett. **68**, 499 (1996).

[44] H. Bracht, N. A. Stolwijk, M. Laube, and G. Pensl, Appl. Phys. Lett. **77**, 3188 (2000).

[45] M. Bockstedte, A. Mattausch, and O. Pankratov, Phys. Rev. B **70**, 115203 (2004).

[46] R. B. Capaz, A. Dal Pino, Jr., and J. D. Joannopoulos, Phys. Rev. B **50**, 7439 (1994).